

A Series of Zn(II) Terpyridine Complexes with Enhanced Two-Photon-Excited Fluorescence for *in Vitro* and *in Vivo* Bioimaging[†]

Qiong Zhang,^{||[a,b]} Xiaohe Tian,^{||[c]} Zhangjun Hu,^{||[b]} Caroline Brommesson,^[b] Jieying Wu,^{*[a]} Hongping Zhou,^[a] Shengli Li,^[a] Jiaxiang Yang,^[a] Zhaoqi Sun,^{*[d]} Yupeng Tian^{*[a,c]} and Kajsa Uvdal^[b]

^{||} These authors contributed equally to this work

^[a] Department of Chemistry, Key Laboratory of Functional Inorganic Materials Chemistry of Anhui Province, Anhui University, Hefei 230039, P. R. China E-mail: yptian@ahu.edu.cn; jywu1957@163.com

^[b] Division of Molecular Surface Physics & Nanoscience, Department of Physics, Chemistry and Biology (IFM), Linköping University, 58183 Linköping (Sweden)

^[c] Department of Chemistry, The MRC/UCL Centre for Medical Molecular Virology, University College London, WC1H 0AJ, London, UK

^[d] School of Physics and Material Science, Anhui University, Hefei 230601, P. R. China E-mail: szq@ahu.edu.cn

^[e] State Key Laboratory of Coordination Chemistry, Nanjing University, Nanjing 250100, P. R. China

Materials and Apparatus.....	5
X-ray Crystallography.....	5
Computational studies.....	5
Optical Measurements.....	6
Two-Photon Excited Fluorescence (TPEF) Spectroscopy and Two-Photon Absorption (2PA) Cross-Section.....	6
Cell Image.....	6
Microscopy.....	7
Cytotoxicity Assays in Cells.....	7
Bioimaging in Zebrafish Larva.....	8
Browser, Zeiss LSM Image Expert and Image J.....	8
Scheme S1. Synthetic routes for the ligands and their metal complexes.....	8
Figure S1. The molecular structures of the ligands and their metal complexes.....	9
Figure S2. Representation of calculated Kohn-Sham orbitals of L ₁ , L ₂ and 1	9
Figure S3. Linear absorption and linear emission spectra of L ₁	9
Figure S4. Linear absorption and linear emission spectra of L ₂	10
Figure S5. Linear absorption and linear emission spectra of 1	10
Figure S6. Linear absorption and linear emission spectra of 2	11
Figure S7. Linear absorption and linear emission spectra of 3	11
Figure S8. Linear absorption and linear emission spectra of 4	12
Figure S9. (a) OPA and OPEF spectra of all compounds in DMF and DMSO.....	12
Figure S10. Lippert–Mataga regressions of the three compounds.....	12
Figure S11. Log–Log linear spectra of L ₁ , 1 , 2 and 4	13
Figure S12. TPEF spectra of all compounds in DMF.....	13
Figure S13. 2PA spectra of all compounds in DMF.....	13
Figure S14. Cytotoxicity data results obtained from the MTT assay.....	14
Figure S15. Cell imaging of L ₂	14
Figure S16. Variable temperature ¹ H NMR of 1 in DMSO- <i>d</i> ₆ /D ₂ O (1:1 v/v).....	15
Figure S17 ¹ H NMR spectra of all the compounds and the mass spectra of 3 and 4	16
Table S1. Crystallographic data and structure refinement for L ₁ , L ₂ , 1 and 2	16
Table S2. Selected intra- and intermolecular bond lengths [Å] and angles [°] for 1 and 2	17
Table S3 Photophysical data of all the compounds.....	18
Reference.....	19

Materials and Apparatus

All chemicals and solvents were dried and purified by usual methods. The synthetic routes for the ligands (**L**₁ and **L**₂) and their metal complexes were illustrated in **Scheme 1**. **L**₁ was obtained by one-step reaction. Through the Solvent-free Wittig reaction, **L**₂ was obtained in high yields. Both the ligands were purified over recrystallization. Elemental analysis was performed with a Perkin–Elmer 240 analyzer. IR spectra (4000–400 cm⁻¹), as KBr pellets, were recorded on a Nicolet FT–IR 170 SX spectrophotometer. Mass spectra were obtained on a Micromass GCT-MS Spectrometer. ¹H and ¹³C NMR spectra were recorded on a Bruker AV 400 spectrometer with tms as internal standard.

X-ray Crystallography

Single-crystal X-ray diffraction measurements were carried out on a Siemens Smart 1000 CCD diffractometer equipped with a graphite crystal monochromator situated in the incident beam for data collection at room temperature. The determination of unit cell parameters and data collections were performed with Mo-K_α radiation ($\lambda = 0.71073 \text{ \AA}$). Unit cell dimensions were obtained with least-squares refinements, and all structures were solved by direct methods with SHELXL-97.¹ All nonhydrogen atoms were located in successive difference Fourier syntheses. The final refinement was performed by full-matrix least-squares methods with anisotropic thermal parameters for non-hydrogen atoms on F^2 . The hydrogen atoms were added theoretically and riding on the concerned atoms.

Computational studies

To better understand the charge transfer state, density functional theory (DFT) calculations on all the compounds were carried out in DMSO. Optimizations were carried out with B3LYP/6-31G(d) and B3LYP[LANL2DZ] without any symmetry restraint². The time-dependent density functional theory (TD-DFT) B3LYP/6-31G(d) and B3LYP-[LANL2DZ] calculations, including optimizations and TD-DFT, were implemented with the G03 software³. Geometry optimization of singlet-singlet excitation energies were carried out with a basis set composed of 6-31G(d) for C, N, S, F, P and H atoms and the LANL2DZ basis set for Zn atoms. The basis set was downloaded from the EMSL basis set library. The lowest 25 spin-allowed singlet-singlet transitions, up to energy of about 5 eV, were taken into account in the calculation of the absorption spectra.

Optical Measurements

The OPA spectra were measured on a UV-3600 spectrophotometer. The OPEF measurements were performed by using an F-2500 fluorescence spectrophotometer. The concentration of sample solution was $1.0 \times 10^{-5} \text{ mol/L}$.

The fluorescence quantum yields (Φ) were determined by using coumarin 307 as the reference according to the literature method ⁴. Quantum yields were corrected as follows:

$$\Phi_S = \Phi_r \left(\frac{A_r(\lambda_r)}{A_s(\lambda_s)} \right) \left(\frac{n_s^2}{n_r^2} \right) \frac{\int F_S}{\int F_r}$$

Where the *s* and *r* indices designate the sample and reference samples, respectively, *A* is the absorbance at λ_{exc} , *n* is the average refractive index of the appropriate solution, and *D* is the integrated area under the corrected emission spectrum⁵. For time-resolved fluorescence measurements, the fluorescence signals were collimated and focused onto the entrance slit of a monochromator with the output plane equipped with a photomultiplier tube (HORIBA HuoroMax-4P). The decays were analyzed by ‘least-squares’. The quality of the exponential fits was evaluated by the goodness of fit (χ^2).

Two-Photon Excited Fluorescence (TPEF) Spectroscopy and Two-Photon Absorption (2PA) Cross-Section

2PA cross-sections (σ) of the samples were obtained by the two-photon excited fluorescence (TPEF) method with a femtosecond laser pulse and a Ti:sapphire system (690–860 nm, 80 MHz, 140 fs) as the light source. The concentration of sample solution was 1.0×10^{-3} M. Thus, the δ values of samples were determined by the following Equation (1). $\delta_s = \delta_r \cdot F_s \cdot \Phi_r \cdot C_r \cdot n_r / F_r \cdot \Phi_s \cdot C_s \cdot n_s$ where the subscripts “s” and “r” represent sample and reference (here, fluorescein in ethanol solution at a concentration of 1.0×10^{-3} mol/L was used as reference), respectively. *F* is the overall fluorescence collection efficiency intensity of the fluorescence signal collected by the fiber spectra meter. Φ , *n* and *c* are the quantum yield of the fluorescence, the refractive index of solvent, and the concentration of the solution, respectively.

Cell Image and Microscopy.

HepG2 cells were seeded in 24-well plates at a density of 5×10^3 cells per well and grown for 96 hours. For live cell imaging, cells were incubated with the complexes (10% PBS: 90% cell media) at the concentrations of 40 μ M and maintained at 37°C in an atmosphere of 5% CO₂ and 95% air for 2 hours. The cells were then washed with PBS (3 x 3 ml per well) and 3 ml of PBS was added to each well. The cells were imaged using confocal laser scanning microscopy with 63X Oil-immersion lenses using ZEISS LSM 710 META upright system, equipped with 650+ two-photon laser excitation source. Excitation wavelength of **1** was 720 nm and the fluorescence emission was measured at 495-582 nm. Cell mitochondria was marked by MitoTracker® Red CMXRos (Life Sciences®, M-7512) at 500nM (in PBS for 10min) excitation wavelength was 546 nm and the fluorescence emission was measured at 560-600 nm. Cell endoplasmic reticulum was marked by ER-Tracker™ Green (BODIPY® FL

Glibenclamide, Life Sciences®, E34251) at 1 μ M (in DMEM for 30min), excitation wavelength was 488 nm and the fluorescence emission was measured at 500-550 nm.

Microscopy.

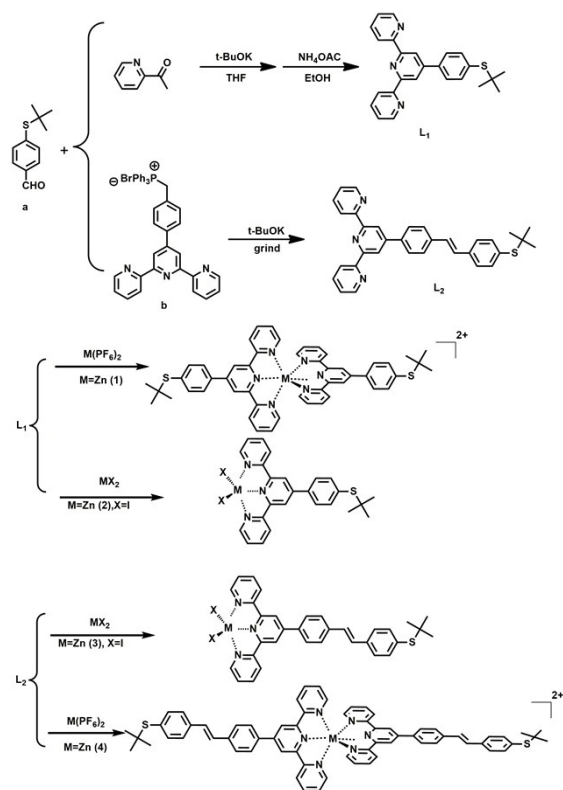
HepG2 cells were imaged on a Zeiss LSM 710 META upright confocal laser scanning microscope using magnification 40 \times and 100 \times water-dipping lenses for monolayer cultures. Image data acquisition and processing was performed using Zeiss LSM Image Browser, Zeiss LSM Image Expert and Image J.

Cytotoxicity Assays in Cells.

To ascertain the cytotoxic effect of all the compounds treatment over a 24h period, the 5-dimethylthiazol-2-yl-2,5-diphenyltetrazolium bromide (MTT) assay was performed. HepG2 cells were trypsinized and plated to \sim 70% confluence in 96-well plates 24 h before treatment. Prior to the compounds' treatment, the DMEM was removed and replaced with fresh DMEM, and aliquots of the compound stock solutions (500 μ M DMSO) were added to obtain final concentrations of 20, 40, 60, 80 and 100 μ M. The treated cells were incubated for 24 h at 37 $^{\circ}$ C and under 5% CO₂. Subsequently, the cells were treated with 5 mg/mL MTT (40 μ L/well) and incubated for an additional 4 h (37 $^{\circ}$ C, 5% CO₂). Then, DMEM was removed, the formazan crystals were dissolved in DMSO (150 μ L/well), and the absorbance at 490 nm was recorded. The cell viability (%) was calculated according to the following equation: cell viability % = $OD_{490}(\text{sample})/OD_{490}(\text{control}) \times 100$, where $OD_{490}(\text{sample})$ represents the optical density of the wells treated with various concentration of the compounds and $OD_{490}(\text{control})$ represents that of the wells treated with DMEM + 10% FCS. Three independent trials were conducted, and the averages and standard deviations are reported. The reported percent cell survival values are relative to untreated control cells.

Bioimaging in Zebrafish Larva

Zebrafish embryos or larvae after fertilization were incubated at 28.5 $^{\circ}$ C in pure water from Milli-Q system. The 3-day-old zebrafish larvae were fed with 30 μ M **1** solution at 28.5 $^{\circ}$ C for 4 h, then the larvae were washed with 1 \times PBS three times at 28.5 $^{\circ}$ C for 20 min. After rinse with 1 \times PBS for three times, the larvae were then embedded in methyl cellulose for imaging. L₂-fed larvae were also imaged for comparison. Image data acquisition and processing was performed using Zeiss LSM Image Browser, Zeiss LSM Image Expert and Image J.



Scheme S1. Synthetic routes for the ligands and their metal complexes.

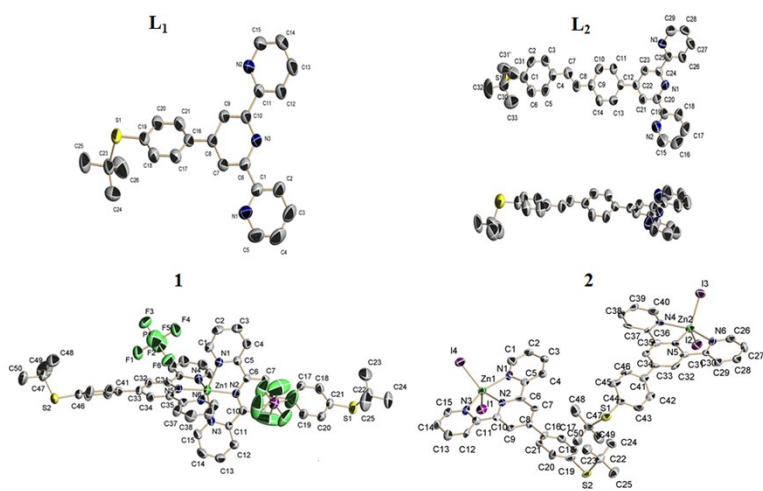


Figure S1. The molecular structures of the ligands and their metal complexes.

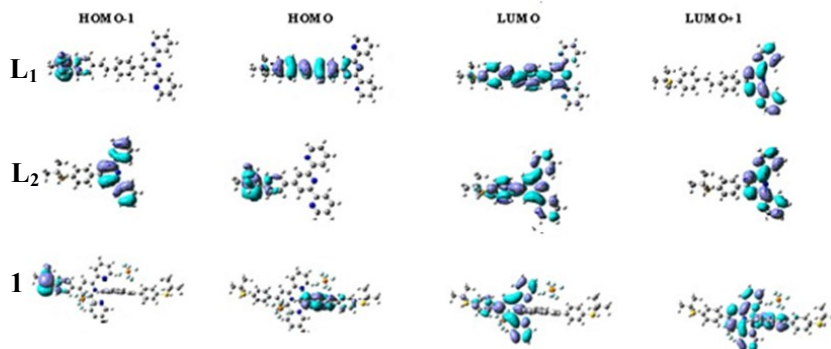


Figure S2. Representation of calculated Kohn-Sham orbitals of L_1 , L_2 and 1

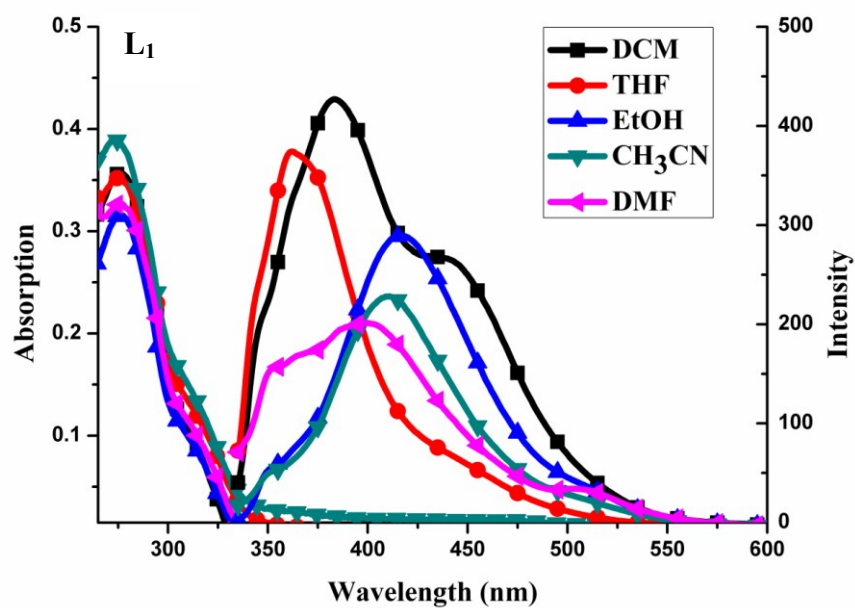


Figure S3. Linear absorption and linear emission spectra of L_1 in five organic solvents with a concentration of 1×10^{-5} mol/L.

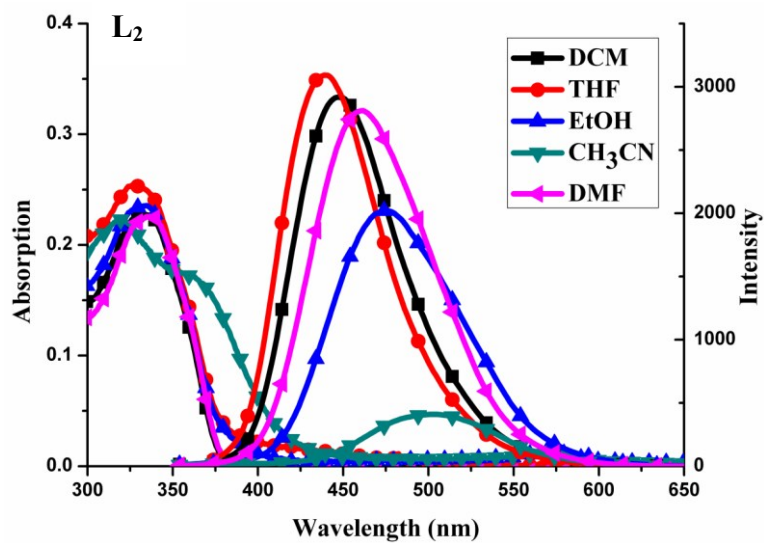


Figure S4. Linear absorption and linear emission spectra of L_2 in five organic solvents with a concentration of 1×10^{-5} mol/L.

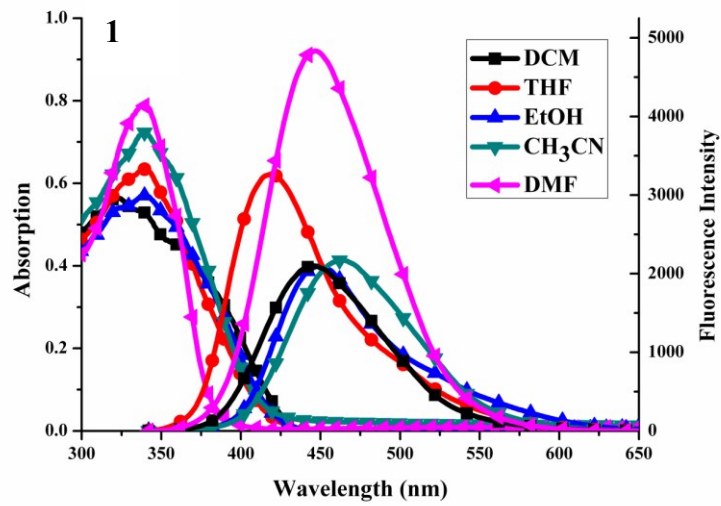


Figure S5. Linear absorption and linear emission spectra of **1** in five organic solvents with a concentration of 1×10^{-5} mol/L.

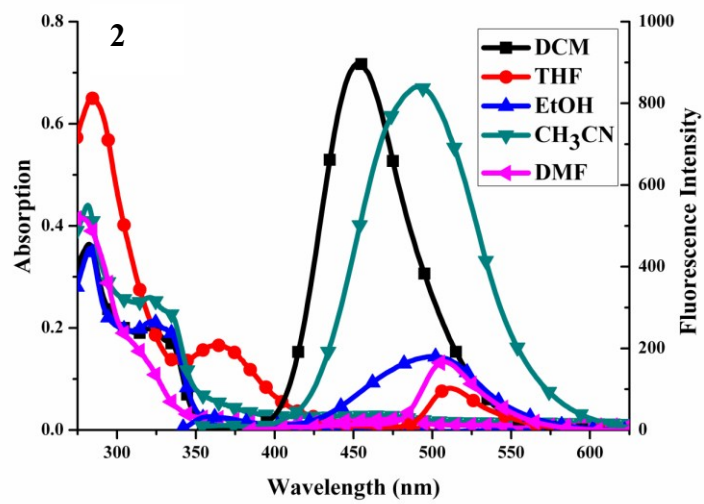


Figure S6. Linear absorption and linear emission spectra of **2** in five organic solvents with a concentration of 1×10^{-5} mol/L.

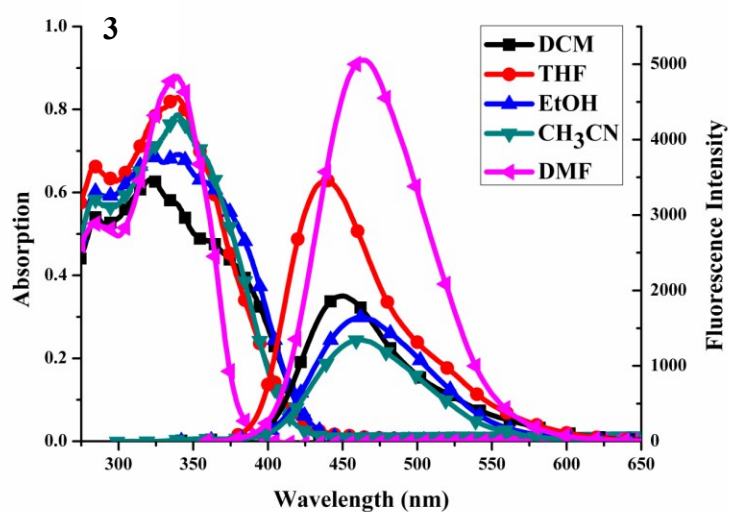


Figure S7. Linear absorption and linear emission spectra of **3** in five organic solvents with a concentration of 1×10^{-5} mol/L.

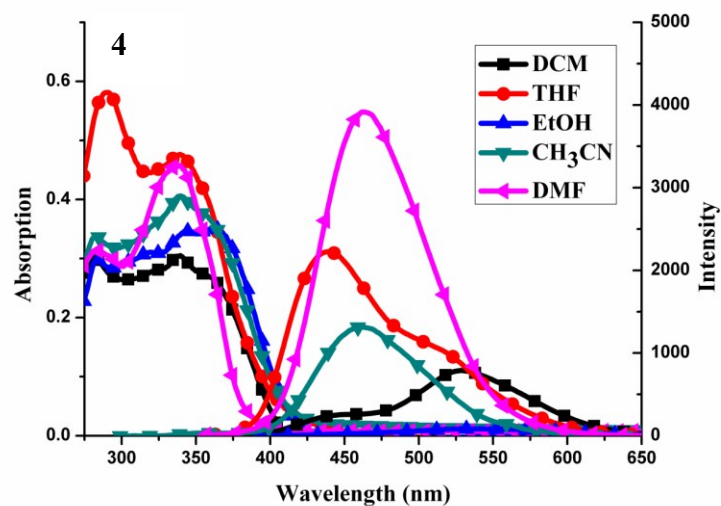


Figure S8. Linear absorption and linear emission spectra of **4** in five organic solvents with a concentration of 1×10^{-5} mol/L.

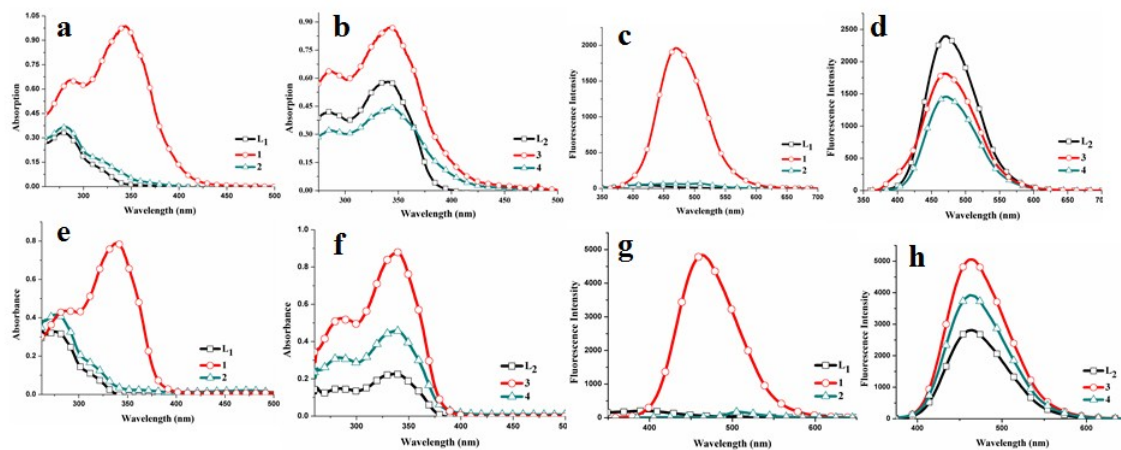


Figure S9. (a) OPA spectra of **L**₁ and **1-2** ($c = 1.0 \times 10^{-5}$ mol L⁻¹) in DMSO/H₂O (1:1,v/v) (b) OPA spectra of **L**₂ and **3-4** in DMSO/H₂O (1:1,v/v) (c) OPEF spectra of **L**₁ and **1-2** in DMSO/H₂O (1:1,v/v) (d) OPEF spectra of **L**₂ and **3-4** in DMSO/H₂O (1:1,v/v) (e) OPA spectra of **L**₁ and **1-2** ($c = 1.0 \times 10^{-5}$ mol L⁻¹) in DMF (f) OPA spectra of **L**₂ and **3-4** in DMF (g) OPEF spectra of **L**₁ and **1-2** in DMF (h) OPEF spectra of **L**₂ and **3-4** in DMF

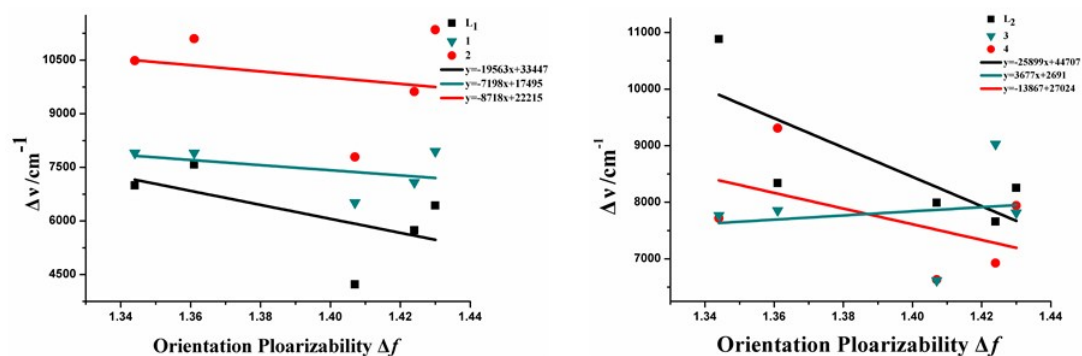


Figure S10. Lippert -Mataga regressions of the three compounds.

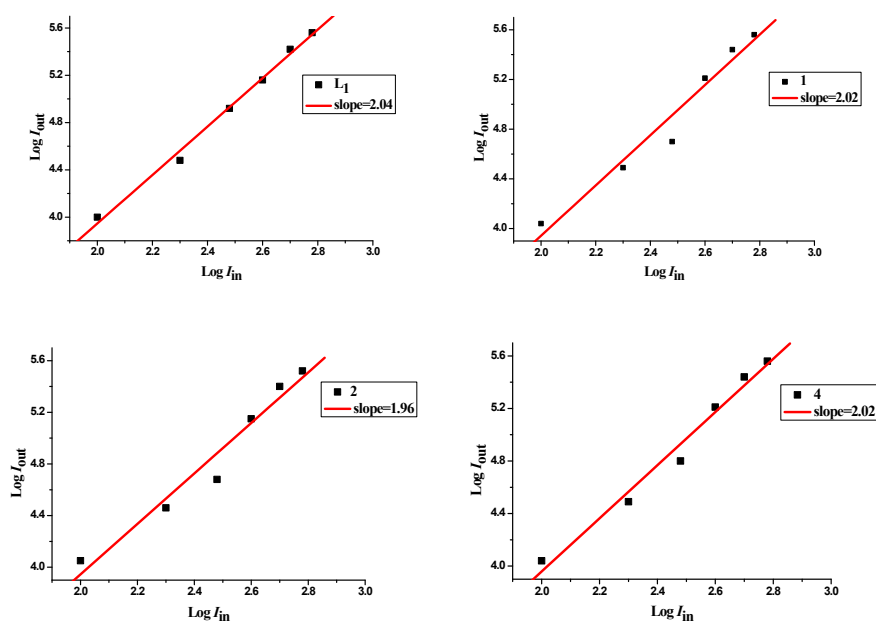


Figure S11. Log-Log linear of squared dependence of induced fluorescence signal and incident irradiance

intensity of two ligands and complexes **L**₁, **1**, **2** and **4**.

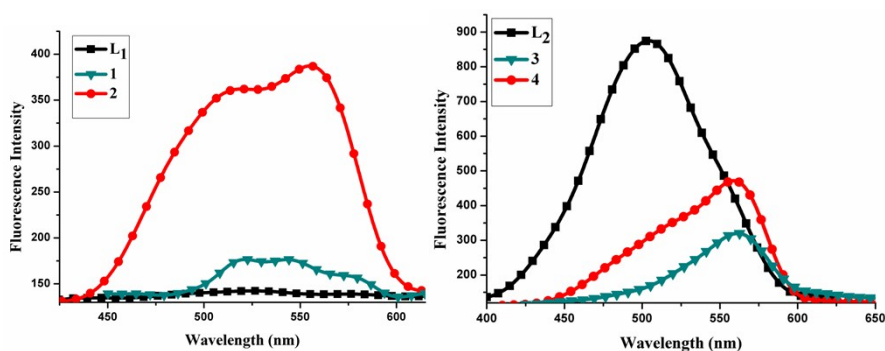


Figure S12. TPEF spectra of all compounds in DMF with $c = 1$ mM at the optimal excitation wavelength.

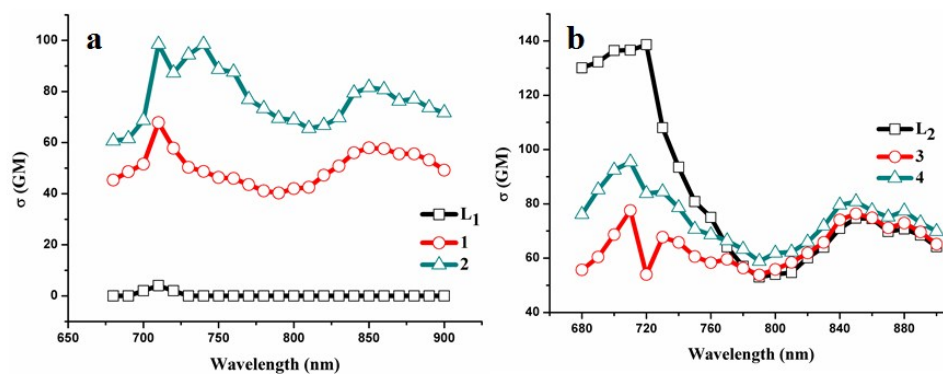


Figure S13. 2PA cross section (σ) spectra of L₁ (a) and L₂ (b) and related complexes

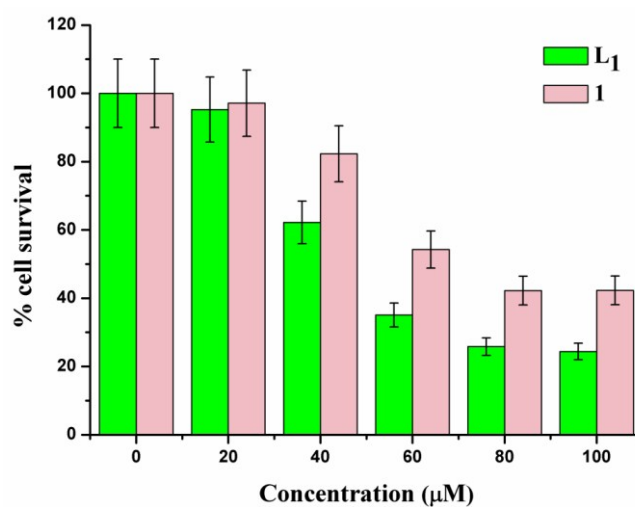


Figure S14. Cytotoxicity data results obtained from the MTT assay.

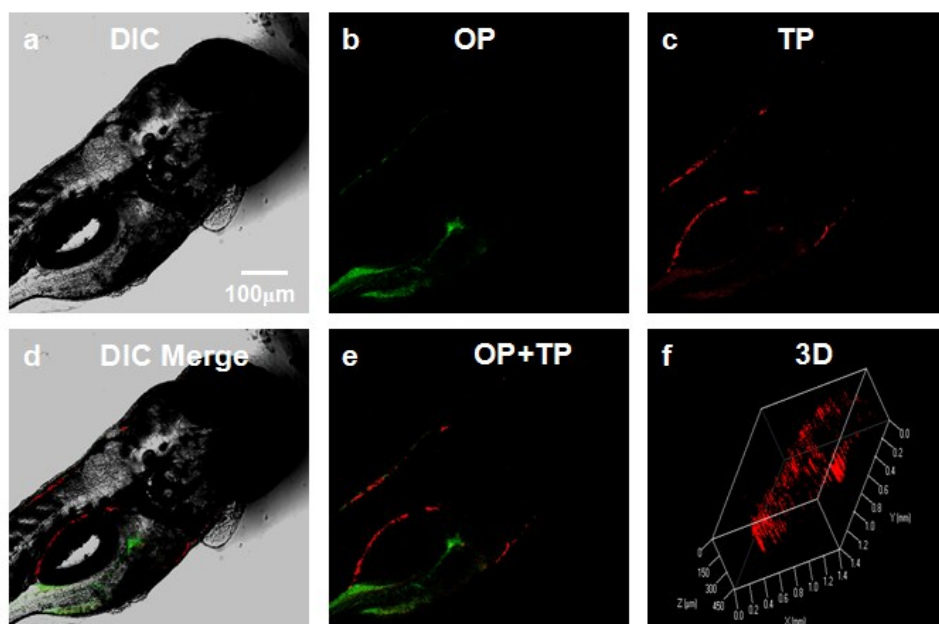


Figure. S15. (a) Bright-field image of 72 h-zebrafish larva. (b) One-photon image of 72 h-zebrafish larva incubated with $60 \mu\text{M}$ L_2 after 4 h of incubation, washed by PBS buffer. $\lambda_{\text{ex}} = 405 \text{ nm}$ (emission wavelength from 350 to 450 nm). (c) Two-photon image of 72 h-zebrafish larva incubated with $60 \mu\text{M}$ L_2 after 4 h of incubation, washed by PBS buffer. $\lambda_{\text{ex}} = 710 \text{ nm}$ (emission wavelength from 500 to 600 nm). (d) zoom of the (b) images. (e) The overlay of (b) and (c). (f) The overlay of (a) to (c). (f) Two-photon excited fluorescence 3D images of zebrafish larva reconstructed from (c)

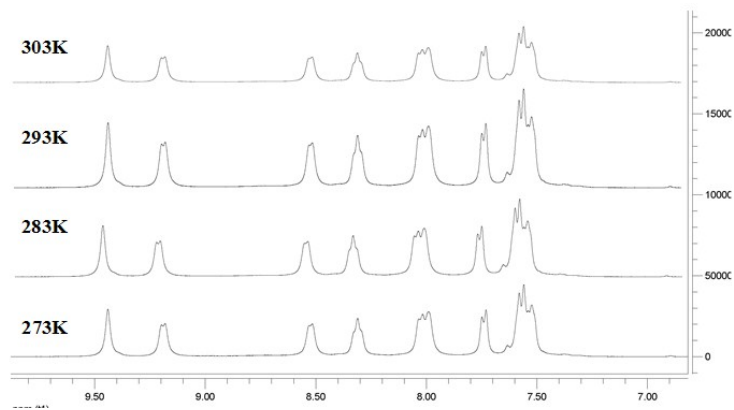
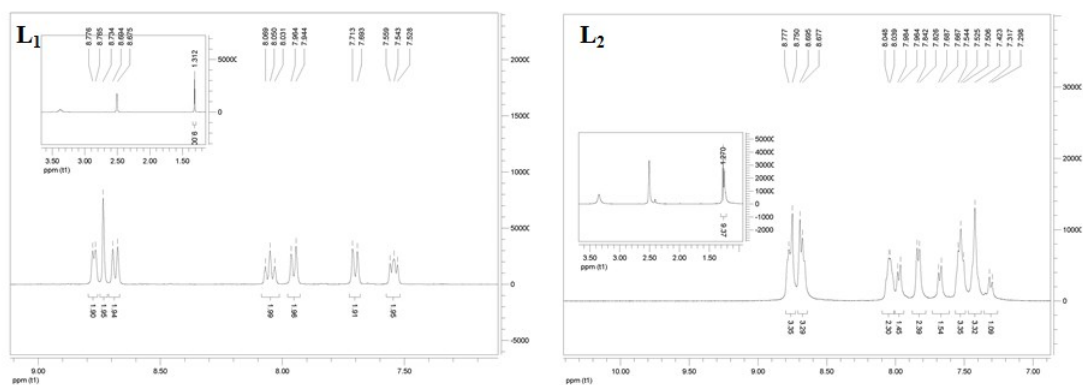


Figure S16. Variable temperature ^1H NMR of **1** in $\text{DMSO-}d_6/\text{D}_2\text{O}$ (1:1 v/v).



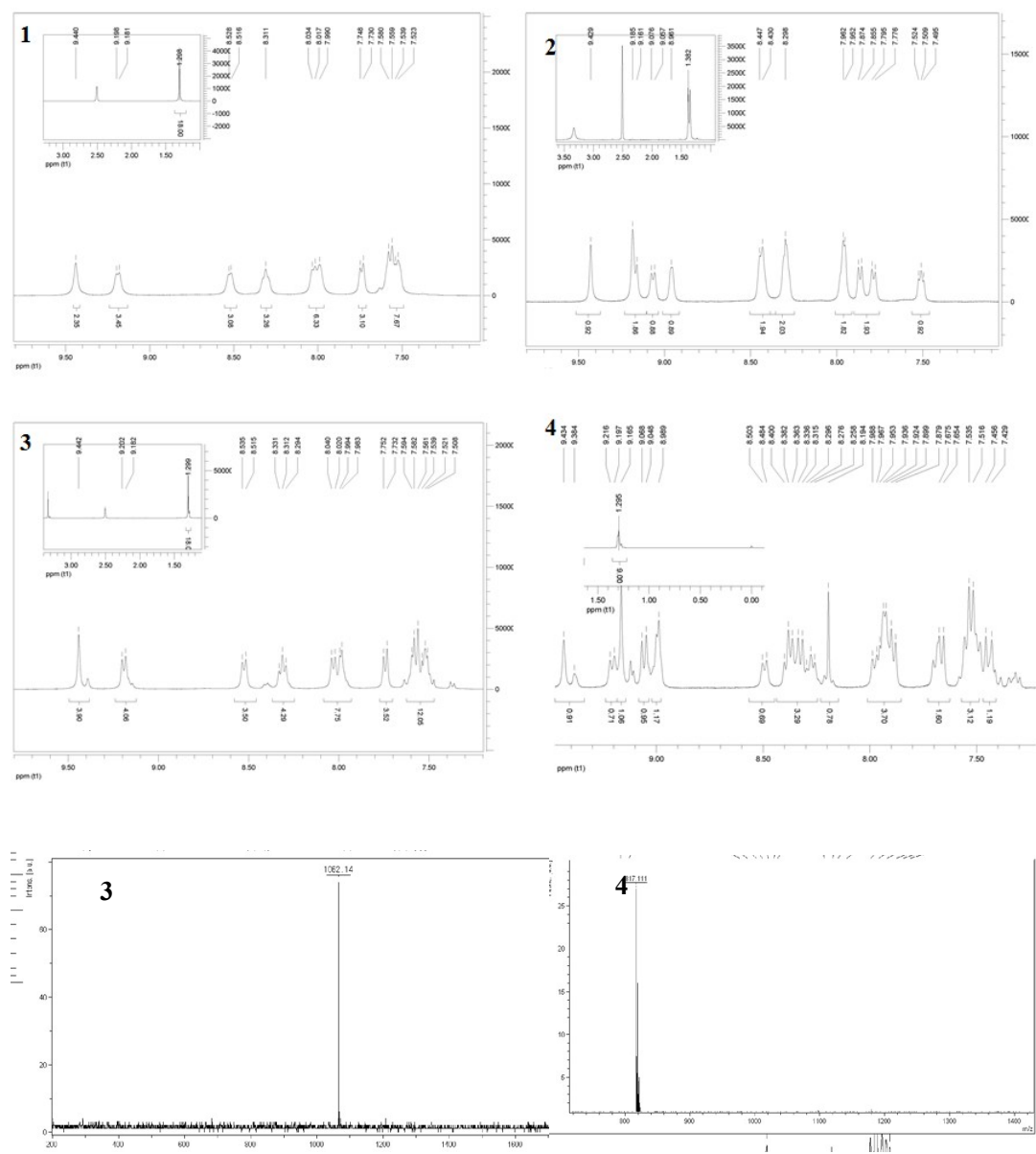


Figure S17 ^1H NMR spectra of all the compounds and the mass spectra of **3** and **4**.

Table S1. Crystallographic data and structure refinement for **L₁**, **L₂**, **1** and **2**.

Compound	L₁	L₂	1	2
CCDC	890206	890205	890201	890203
formula	$\text{C}_{25}\text{H}_{23}\text{N}_3\text{S}$	$\text{C}_{33}\text{H}_{29}\text{N}_3\text{S}$	$\text{C}_{50}\text{H}_{46}\text{F}_{12}\text{N}_6\text{P}_2$ S_2Zn	$\text{C}_{25}\text{H}_{23}\text{I}_2\text{N}_3\text{S}$ Zn
Formula weight	397.52	499.65	1150.36	716.69
T/K	293(2)	298(2)	298(2)	296(2)

$\lambda(\text{Mo-K}\alpha)$ Å	0.71073	0.71073	0.71069	0.71073
crystal system	Triclinic	Monoclinic	Monoclinic	triclinic
space group	$P\bar{1}$	$P2_1/c$	$P2_1/c$	$P\bar{1}$
$a/\text{Å}$	8.2244(16)	38.020(17)	19.299(5)	14.035(4)
$b/\text{Å}$	10.228(2)	12.719(6)	16.646(5)	14.277(4)
$c/\text{Å}$	14.193(3)	11.416(5)	16.423(5)	15.099(5)
α/deg	70.91(3)	90		63.305(3)
β/deg	81.49(3)	96.376(7)	103.90 (5)	79.986(4)
γ/deg	72.81(3)	90		84.168(4)
$V/\text{Å}^3$	1076.1(4)	5486(4)	5121(3)	2661.0(14)
$D_c/\text{Mg m}^{-3}$	1.227	1.210	1.492	1.789
Z	2	8	4	4
$F(000)$	420	2112		1384
μ/mm^{-1}	0.166	0.144	0.709	3.339
reflections collected	9269	26538	35052	18616
reflections unique	4228	9486	11198	9224
$R(\text{int})$	0.0155	0.1063	0.1188	0.1039
data/restrain	4228 / 0 /	9486 / 186 /		9224 / 6 /
ts/params	265	696		577
Final R			$R_I=0.0705$	$R_I=0.0654$
indices[$I>2$]	$R_1=0.0450$ $wR_2=0.1471$	$R_I=0.0791$ $wR_2=0.0624$	$wR_2=0.1601$	$wR_2=0.1399$
$\sigma(I)$				
GOF on F^2	1.003	1.068	0.961	0.980

Table S2. Selected intra- and intermolecular bond lengths [Å] and angles [°] for **1** and **2**.

1					
Zn1-N2	2.063(4)	Zn1-N5	2.062(4)	Zn1-N6	2.161(5)
Zn1-N4	2.170(5)	Zn1-N1	2.168(5)	Zn1-N3	2.235(5)
N2-Zn1-N5	174.73(18)	N2-Zn1-N6	105.37(18)	N2-Zn1-N1	75.97(17)
N6-Zn1-N3	85.77(18)	N1-Zn1-N3	151.12(16)	N5-Zn1-N6	75.90(18)
N5-Zn1-N1	108.97(17)	N6-Zn1-N1	100.09(17)	N2-Zn1-N3	75.21(17)
N6-Zn1-N4	151.70(16)	N1-Zn1-N4	87.76(18)	N5-Zn1-N3	99.89(17)
2					
I(1)-Zn(1)	2.5770(19)	Zn(1)-N(1)	2.211(10)	N(3)-Zn(1)-N(1)	148.4(3)

I(2)-Zn(2)	2.586(2)	Zn(2)-N(5)	2.076(11)	N(2)-Zn(1)-I(4)	130.0(3)
I(3)-Zn(2)	2.5689(18)	Zn(2)-N(4)	2.177(10)	N(3)-Zn(1)-I(4)	96.4(3)
I(4)-Zn(1)	2.5541(19)	Zn(2)-N(6)	2.201(10)	N(1)-Zn(1)-I(4)	99.2(3)
Zn(1)-N(2)	2.109(9)	N(2)-Zn(1)-N(3)	74.3(4)	N(2)-Zn(1)-I(1)	111.0(3)
Zn(1)-N(3)	2.176(10)	N(2)-Zn(1)-N(1)	74.6(4)	N(3)-Zn(1)-I(1)	100.1(3)
I(1)-Zn(1)	2.5770(19)	Zn(1)-N(1)	2.211(10)	N(3)-Zn(1)-N(1)	148.4(3)

Table S3 Photophysical data of all the compounds

	Solvents	λ_{\max}^a	ϵ^b	λ_{\max}^c	Φ^d	λ_{\max}^e	λ_{\max}^f	δ^g	τ^h	$\Delta\nu/cm^{-1}$	$\Delta\mu^i$
L₁	DCM	274	3.6	383	0.29	510	710	5	0.42	5737	3.22
		314	0.98						0.13	4222	
	THF	275	3.5	362	0.13				0.13	4222	
		314	1.2						1.53	7575	
	EtOH	275	3.2	412	0.19				0.13	6993	
		314	1.2						0.22	6429	
	CH ₃ CN	274	3.8	404	0.13				0.22	6429	
		315	1.4						1.10	7658	
DMF	276	3.3	395	0.16	0.52	7990					
	315	1.0			0.15	8338					
L₂	DCM	280	1.7	447	0.65	562	720	139	1.10	7658	5.27
		333	2.3						0.52	7990	
	THF	282	2.4	439	0.61				0.15	8338	
		325	2.5						1.54	10883	
	EtOH	281	1.8	461	0.52				0.12	10883	
		333	2.3						1.56	8252	
	CH ₃ CN	287	1.9	491	0.12				1.56	8252	
		320	2.2						1.17	7077	
DMF	282	1.5	463	0.70	1.17	7077					
	335	2.3			1.09	6510					
1	DCM	283	4.7	446	0.22	558	710	97	1.17	7077	4.35
		339	5.7						1.09	6510	
	THF	283	4.8	435	0.29				0.14	7900	
		339	6.4						0.23	7900	
	EtOH	283	4.2	463	0.23				0.14	7900	
		339	5.7						1.54	7900	
	CH ₃ CN	283	5.2	463	0.17				1.54	7900	
		339	7.2						1.56	7946	
DMF	283	4.3	464	0.34	1.56	7946					
	339	7.9			2.56	9619					
2	DCM	277	3.6	454	0.20			2.56	9619		

		316	2.0							
		284	6.6					1.02	7789	
	THF	365	1.6	510	0.02					
		283	3.5					1.75	11101	3.29
	EtOH	324	2.1	506	0.05					
		281	4.4					1.17	10485	
	CH ₃ CN	325	2.5	493	0.20					
		281	4.2		0.03	528	710	65	0.64	11350
	DMF	321	1.6	505	6					
3		284	5.4					2.86	9027	
	DCM	320	6.3	450	0.18					
		284	6.7	437	0.09			0.99	6615	
	THF	339	8.3							
		284	6.0		0.18			0.44	7853	3.32
	EtOH	339	6.9	462						
		281	5.8					1.27	7766	
	CH ₃ CN	340	7.8	462	0.24					
		284	5.2			558	710	95	1.57	7813
	DMF	340	8.9	463	0.32					
4		281	3.0					1.03	6925	
	DCM	339	3.0	443	0.19					
		290	5.9	439	0.31			1.17	6632	
	THF	340	4.8							
		282	2.9					0.41	9309	4.77
	EtOH	362	3.4	546	0.02					
		281	3.4					1.54	7719	
	CH ₃ CN	340	4.1	461	0.19					
		283	3.1			563	710	77	1.53	7940
	DMF	338	4.6	462	0.48					

^a Absorption peak position in nm (1×10^{-5} mol L⁻¹). ^b Maximum molar absorbance in 10^4 mol⁻¹ L cm⁻¹. ^c Peak position of SPEF in nm (1.0×10^{-5} mol L⁻¹), excited at the absorption maximum. ^d Quantum yields determined by using coumarin 307 ($\Phi = 0.56$) (1.0×10^{-5} mol L⁻¹) as the standard. ^e TPEF peak position in nm pumped by femtosecond laser pulses at 300 mw at their maximum excitation wavelength. ^f 2PA maximum excitation wavelength. ^g 2PA cross section in GM. ^h The fitted fluorescence lifetime in ns. ⁱ fluorescence lifetime (ns). ^j Stokes shift in cm⁻¹. ^k $\Delta\mu$ the dipole moment changes of the compounds with photoexcitation ($1D=3.334 \times 10^{-30}$ c·m).

Reference

- (1) Holland, J. P.; Aigbirio, F. I.; Betts, H. M.; Bonnitcha, P. D.; Burke, P.; Christlieb, M.; Churchill, G. C.; Cowley, A. R.; Dilworth, J. R.; Donnelly, P. S.; Green, J. C.; Peach, J. M.; Vasudevan, S. R.; Warren, J. E. Functionalized Bis(thiosemicarbazone) Complexes of Zinc and Copper: Synthetic Platforms Toward Site-Specific Radiopharmaceuticals. *Inorg. Chem.* **2007**, *46*, 465–485.
- (2) Ji, Z. Q.; Li, Y. J.; Pritchett, T. M.; Makarov, N. S.; Haley, J. E.; Li, Z. J.; Drobizhev, M.; Rebane, A. and Sun, W. F. One-Photon Photophysics and Two-Photon Absorption of 4-[9,9-Di(2-ethylhexyl)-7-diphenylamino]fluoren-2-yl]-2,2':6',2''-terpyridine and Their Platinum Chloride Complexes. *Chem. Eur. J.* **2011**, *17*, 2479–2491.
- (3) Zheng, Q.; He, G. S.; Prasad, P. N. Novel two-photon-absorbing, 1,10-phenanthroline-containing π -conjugated chromophores and their nickel(II) chelated complexes with quenched emissions. *J. Mater. Chem.* **2005**, *15*, 579–587.
- (4) Demas, J. N. and Crosby, G. A. Measurement of photoluminescence quantum yields. Review. *J. Phys. Chem.*, **1971**, *75*, 991–1024.

(5) Gray, T. G.; Rudzinski, C. M.; Meyer, E. E.; Holm, R. H and Nocera, D. G. Spectroscopic and Photophysical Properties of Hexanuclear Rhenium(III) Chalcogenide Clusters. *J. Am. Chem. Soc.*, **2003**, 125, 4755-4770.